J Solid State Electrochem (2016) 20:3015–3023
DOI 10.1007/s10008-016-3266-8

ORIGINAL PAPER

Pd-modified PEDOT layers obtained through electroless metal deposition—electrooxidation of glycerol

Maria Ilieva[1] · **Aneliya Nakova**[1] · **Vessela Tsakova**[1]

Received: 31 March 2016 / Revised: 25 May 2016 / Accepted: 30 May 2016 / Published online: 18 June 2016

Abstract Pd-poly(3,4-ethylenedioxythiophene) (PEDOT)-based electrocatalytic materials are obtained by coupling Pd ion reduction with oxidation of pre-reduced PEDOT coatings. Electroless metal deposition is carried out in single or triple electroless deposition steps resulting in Pd NPs with mean size ranging between 12 and 22 nm, respectively. The proposed method of dispersing the Pd catalytic phase provides the opportunity to obtain high electrocatalytic currents with Pd loadings as low as 10 μg cm^{-2}. The Pd-PEDOT catalyst obtained by triple-step metal deposition shows stable voltammetric behavior with respect to glycerol oxidation in alkaline solution. The established mass activity is between the highest values achieved at Pd-electrocatalysts without involving additional electrocatalytic materials or special supports.

Keywords PEDOT · Pd · Glycerol · Electroless deposition

Introduction

The development of suitable electrocatalysts for direct alcohol fuel cells continues to be the subject of numerous studies [1–4]. Much effort is put into the development of various Pd-based electrocatalytic materials [5–18] due to the prospect to reduce the platinum content in fuel cells. Comparative studies of Pt- and Pd-supported nanoparticles (NPs) have shown that the onset potential for glycerol oxidation is lower on Pt-based catalysts, but nevertheless, in specific experimental conditions, higher oxidation currents are observed on Pd-based materials [8, 10]. It was found that electrooxidation of glycerol may be significantly enhanced by using electrochemically treated palladium surfaces [9]. Different ways of reducing the palladium content and increasing the electroactive surface area were explored such as galvanic replacement of electrochemically deposited copper by palladium [13], formation of two-dimensional assemblies of Pd NPs [14], or use of Pd-decorated core-shell nanocatalysts [16]. Further improvements in terms of electrocatalytic activity were sought by combining Pd with other metals, e.g., Au and Ni [7] or adatoms of Sb, Pb, and Sn [15]. Apart from the metal catalytic centers, the catalyst support is also of utmost importance for the stability and effectiveness of the electrocatalytical performance [6, 11, 12, 17]. Conducting polymers (CP) present one of the possibilities for using supports with high conductivity and well-developed surface area. CP-based supports with deposited Pd particles were investigated as electrocatalysts for alcohol oxidation in various cases [19–28]. Most of the studies [23–28] use poly(3,4-ethylenedioxythiophene), PEDOT, as conducting polymer support, which is known for its stability in alkaline solutions. With one exception [23], PEDOT-based investigations carried out so far involve either massively deposited Pd (or Pd-Ru) dendrite structures [25–27] or graphene as additional composite component [24, 28]. Electrophoretically deposited thin Pd NPs-PEDOT composite layers studied in [23] show enhanced electroactivity for ethanol electrooxidation.

There are different ways of depositing metal particles on conducting polymer materials including chemical and electrochemical approaches [29, 30], e.g., polymerization in the

Dedication This paper is dedicated to Professor György Inzelt on the occasion of his 70th birthday with the appreciation of his long-lasting involvement and strong impact on the development of modern electrochemistry.

✉ Maria Ilieva
milieva@ipc.bas.bg

[1] Institute of Physical Chemistry, Bulgarian Academy of Sciences, 1113 Sofia, Bulgaria

presence of pre-synthesized metal nanoparticles, one-pot chemical synthesis of metal-CP composites, and metal electro- or electroless deposition on pre-deposited CP layers. Electroless metal deposition is carried out either in the presence of solute reductant species (e.g., $NaBH_4$) or at the expanse oxidation of pre-reduced CPs. In the latter case, the CP-coated electrodes are kept at potentials negative enough with respect to the equilibrium potential of the depositing metal ions. It is well understood that the different ways of depositing metallic particles result in very different characteristics (number, size and size distribution and location) of the electrocatalytic phase. Pd electroless deposition (at the expense of CP oxidation) was studied in the case of polyaniline [31–33] and PEDOT [34–38], and the obtained electrocatalysts were tested for oxidation of hydrazine [32, 38] and reduction of hydrogen peroxide [37] and nitrate ions [34]. The investigations on the electroless deposition of Pd on PEDOT [34–38] show that this approach is a suitable way of obtaining well-dispersed metallic phase. Studies using PEDOT-supported Pd NPs carried out in neutral solutions [38] give evidence for the possibility to use these materials for amperometric determination of hydrazine.

Pd-PEDOT coatings were already involved as electrocatalysts for alcohol oxidation in alkaline media. The electrocatalytic materials were obtained by chemical one-pot synthesis [23, 28], metal electrodeposition [25–27], and chemical metal deposition in the presence of $NaBH_4$ [24]. In a former study [22], we have investigated the possibility to use polyaniline (PANI) as a sacrificial layer employed for the deposition of the metallic phase. The Pd-PANI-coated electrode was further subjected to temperature treatment at 400 °C used to decompose the polymer backbone and obtain highly dispersed catalysts deprived from the intrinsic electroactivity of PANI. In the present investigation, we explore the possibility to obtain effective Pd-PEDOT-based electrocatalytic material for glycerol oxidation by electroless deposition of Pd particles on pre-reduced PEDOT coatings. In contrast to former studies on electrooxidation of glycerol by means of electrodeposited Pd dendrites, covering almost completely the PEDOT surface [25–27], the present approach provides the opportunity for fine dispersion of Pd nanoparticles and presents a way of reducing the amount of Pd used in the electrocatalytic material. Glycerol is chosen as a prospective alcohol fuel due to its low toxicity, weak corrosivity, and high boiling point. Moreover, glycerol is obtained as a by-product in the manufacturing of biodiesel which is a further reason for the interest in its conversion as a fuel [39].

Experimental

All electrochemical experiments were carried out in three electrode cells by using a glassy carbon electrode GC (Sigradur®) with surface area $S = 0.08$ cm^2, a platinum plate counter electrode, and a mercury/mercury sulfate reference electrode (MSE) Hg/Hg_2SO_4/0.5 mol cm^{-3} K_2SO_4. The potentials in the text are referred to MSE $E_{MSE/K2SO4} = 0.66$ V versus SHE. Before the experiments, the GC electrode surface was treated with emery cloth (Buehler P4000) and then mirror polished with Al_2O_3 on a Mastertex (Buehler) polishing cloth. The electrolyte solutions were prepared with deionized water ($\rho = 18.2$ MΩ cm) obtained from a Millipore Synergy™ Ultrapure Water Purification System and were de-aerated with argon for at least 30 min before the onset of the electrochemical measurements. A computer-driven potentiostat/galvanostat (Autolab PGSTAT 12; Ecochemie, The Netherlands) was used for the electrochemical experiments.

Each experimental series consisted of several measurements performed consecutively in six electrochemical cells:

1. Electrochemical polymerization of EDOT was carried out in aqueous solution consisting of 0.01 mol cm^{-3} EDOT and 0.1 mol cm^{-3} $LiClO_4$ (Aldrich) at constant anodic potential, $E_a = 0.38$ V. PEDOT films with polymerization charges between 4.4 and 4.9 mC were used in this study. These polymerization charges correspond to thin layers (0.23–0.26 μm) estimated on a 240 mC cm^{-2} polymerization charge per 1 μm thickness basis [34].
2. After synthesis, the polymer-coated electrodes were transferred in supporting electrolyte (0.1 mol cm^{-3} $LiClO_4$) to measure their electroactivity by cyclic voltammetry between −0.66 and +0.32 V. In the same electrolyte, the polymer layers were electrochemically reduced by keeping the working electrode at constant potential, $E = -1.4$ V, for 1200 s.
3. Electroless deposition of palladium nanoparticles (NPs) was carried out by dipping the pre-reduced PEDOT layers in an aqueous solution of 0.002 mol cm^{-3} $PdSO_4$ (Sigma Aldrich) and 0.5 mol cm^{-3} H_2SO_4. The equilibrium potential of Pd^{2+}/Pd in this solution ($E^0_{Pd^{2+}/Pd^0} = 0.195$ V) is positive enough with respect to the potential used for reduction of the PEDOT layers. The electroless deposition process was monitored through the change in the open circuit potential (OCP) of the PEDOT-coated electrode. The process was stopped at $E_{OCP} = -0.05$ V. In some experiments, the electroless deposition step was repeated three times in order to increase the amount of the deposited metal phase. In these cases, the Pd-PEDOT-coated electrode was pre-reduced also before the second and the third electroless deposition step.
4. Reference measurements were completed in alkaline supporting electrolyte (0.5 mol cm^{-3} KOH), in the absence of glycerol, by cyclic voltammetry in order to reveal the existence and electroactivity of the deposited palladium NPs. This experiment was used to determine the

reduction charge of the surface PdO layer and evaluate the electrochemical surface area of the Pd electrocatalyst. A reference value of 424 μC cm^{-2} monoatomic layer of PdO was used in the calculations [40, 41].

5. Electrooxidation of glycerol was studied in the presence of 0.1 mol $cm^{-3}$and 0.5 mol cm^{-3} M glycerol in 0.5 M KOH by cyclic voltammetry for assessing the electrocatalytic activity of the Pd/PEDOT-coated electrodes.
6. Anodic voltammetric stripping of Pd was completed in 1.15 mol cm^{-3} HCl aqueous solution in order to determine the mass of the deposited Pd catalyst.

Scanning electron microscopy (SEM) imaging and energy dispersive x-ray (EDX) analysis was accomplished by means of an SM 6380 (JEOL) apparatus equipped with an INCA Oxford 7582 system.

Results and discussion

In the potential range where electrooxidation of glycerol is expected to take place, PEDOT is in the oxidized, high-conducting state. In voltammetric experiments, in the absence of solute oxidizing/reducing species, PEDOT shows pseudocapacitive charging/discharging behavior with intrinsic currents proportional to the thickness of the CP layer. In order to reduce the contribution of the intrinsic capacitive currents of PEDOT in the electrocatalytic measurements, in the present study, relatively thin PEDOT layers were used as supports for the electrocatalytic metal NPs. This enforced the application of a more negative reduction potential ($E = -1.4$ V) for the pre-treatment of the polymer layers in comparison to former studies on electroless Pd deposition on PEDOT [34–36]. At this potential, the transition of PEDOT from high-to-low conducting state [42, 43] is already initiated (Fig. 1—solid line). The pre-treatment procedure allowed transferring the polymer-coated electrode to the Pd-plating solution by preserving the reduced state of PEDOT.

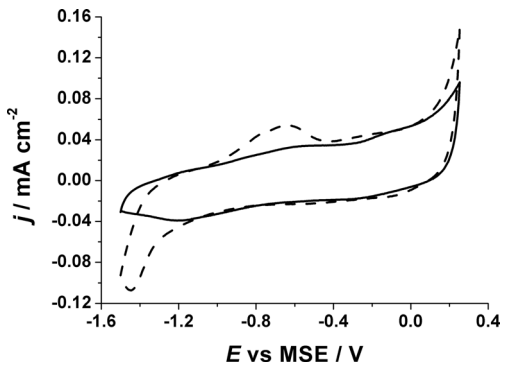

Fig. 1 Cyclic voltammetric curves measured in 0.1 mol cm^{-3} $LiClO_4$ at PEDOT-coated electrode before (*solid line*) and after (*dashed line*) single-step electroless deposition of Pd

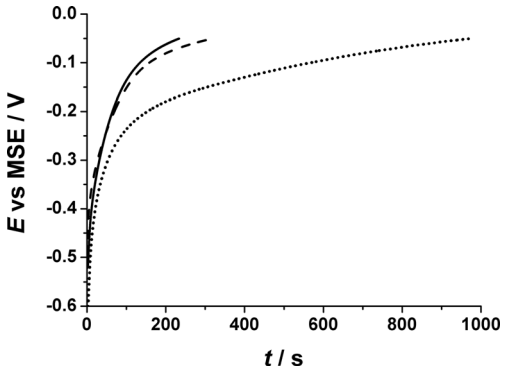

Fig. 2 OCP transients measured in 0.002 mol cm^{-3} $PdSO_4$ and 0.5 mol cm^{-3} H_2SO_4 in the course of a triple-step electroless deposition procedure: first step (*dotted line*), second step (*dashed line*), and third step (*solid line*)

OCP curves measured in the course of three consecutive Pd electroless deposition steps carried out at one and the same PEDOT-coated electrode are shown in Fig. 2. (The PEDOT layer was pre-reduced before each deposition step.) The OCP transient obtained at the pristine PEDOT layer shows a slow increase of potential whereas in subsequent Pd deposition steps, the potential increase is much faster. According to Fig. 1 (dashed line) at the reduction potential ($E = -1.4$ V), Pd-PEDOT reduction takes place together with hydrogen absorption in Pd. Thus, the oxidative transition of the Pd-PEDOT-coated electrodes occurring in the second and third electroless deposition steps involves both PEDOT oxidation and hydrogen desorption. Both processes provide electrons for the reduction of the Pd^{2+} ions available in the solution. Therefore, the Pd particles existing already on the PEDOT layer promote the metal ion reduction in subsequent electroless deposition steps. Metal particles size rather than increase in the number of deposited particles increase should be expected.

The amount of deposited Pd was monitored through anodic voltammetric stripping (Fig. 3). Two stripping peaks are observed with the main one corresponding to the expected potential for the formation of $[PdCl_2]^{4-}$ complex [44]. The

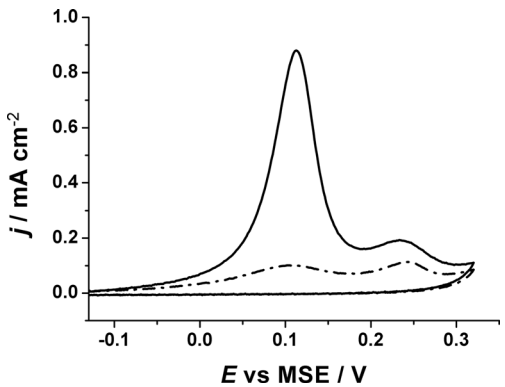

Fig. 3 Anodic dissolution of Pd in 1.15 mol cm^{-3} HCl aqueous solution after single step (*dash dotted line*) and triple-step (*solid line*) electroless deposition. Scan rate $v = 0.005$ V s^{-1}

Table 1 Data for the Pd deposit and electrocatalytic activity of different Pd-PEDOT specimens

Specimen number	Pd deposition	*m* (Pd) (μg cm^{-2})	*q* (PdO) (mC cm^{-2})	*d* (Pd NP) (nm)	Scan rate (V s^{-1})	Glycerol (mol cm^{-3})	*MA* (mA mg^{-1})	j_f/j_b
1	Single	2.82	0.48	12	0.02	0.1	253	2.0
2	Triple	9.37	1.09	18	0.02	0.1	153	2.3
3	Triple	11.09	1.07	22	0.05	0.1	279	2.5
4	Triple	10.34	1.02	22	0.05	0.5	719	2.7
5	Triple	9.65	1.05	20	0.05	0.5	720	2.8

second, more positive stripping peak has a large relative contribution after the first electroless deposition step when the overall Pd content is small. After subsequent electroless deposition steps and corresponding increase in the deposited metal mass, the first stripping peak becomes dominating. It is worth noting that anodic stripping of palladium has the same pattern even if the electrocatalyst was not exposed to glycerol. Thus, the origin of the second stripping peak could not be sought in partial surface contamination of the Pd catalyst. It can be suggested that it is a result of the interaction between the PEDOT chains and Pd species with the largest contribution of the corresponding contact area at low Pd amounts. In fact, it was found that Pd ions interact strongly with (aromatic) thiophenic compounds and $PdCl_2$ was used for selectively slowing down the elution of sulfuric compounds relative to hydrocarbons on chromatographic assays [45].

The amount of deposited metal in the three-step Pd deposition procedure is about four times larger than in the initial Pd electroless deposition step (see Table 1). On the other hand, the surface area of the Pd phase, which is proportional to the charge under the PdO reduction peak, changes by about two times (Table 1). It is worth noting that the deposited electrocatalyst mass (m) to surface area (S) ratio ($m = \rho N(2/3)\pi r^3$, $S = N2\pi r^2$ where N is the number of deposited metal particles, r—their mean radius, and ρ—the density of Pd) is proportional to the linear size of the Pd particles. This ratio increases about twice at triple electroless deposition, and thus the average size of the Pd particles is expected to be doubled. An estimation of the mean size for both cases is made based on the data for the deposited mass and surface area of Pd and results in 12 and 20 nm for the single- and triple-step deposition, respectively.

The direct observation of the Pd-PEDOT catalysts by means of SEM (Fig. 4) shows an even distribution of Pd particles on the polymer surface. The size of the largest particles (or particles agglomerates) is estimated to be about 40 nm in diameter for the specimen with triple electroless deposition of Pd. The used SEM device did not allow a better imaging of the Pd particles, especially on the specimen with a single electroless deposition step. EDX analysis of Pd carried out at Pd-PEDOT-coated electrodes with single and triple step deposition gave a 1:4 ratio of the Pd content for the single- to triple-step deposition specimens which is in line with the results from the electrochemical stripping (Table 1).

The voltammetric behavior of the Pd-PEDOT-coated electrodes in the presence of glycerol is shown in Fig. 5 for specimens obtained by single- and triple-step metal deposition. In both cases, characteristic voltammograms for glycerol oxidation are observed with main forward glycerol oxidation peaks and backward oxidation peaks, the latter ascribed to removal of incompletely oxidized carbonaceous species obtained in the course of glycerol oxidation. Nevertheless, both specimens show different trends in the evolution of the voltammetric behavior in consecutive scans. In the case of Pd-PEDOT (single-step deposition), the main peak gradually decreases and loses about 30 % from the maximal peak current value (Fig. 5a) whereas the triple-step deposition specimen shows a marked increase in the main oxidation peak by more than

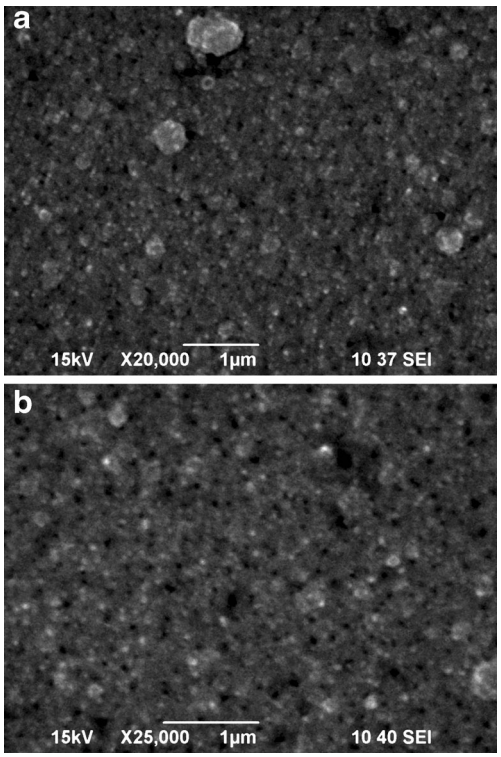

Fig. 4 SEM of Pd-PEDOT specimen obtained by triple-step electroless deposition of Pd

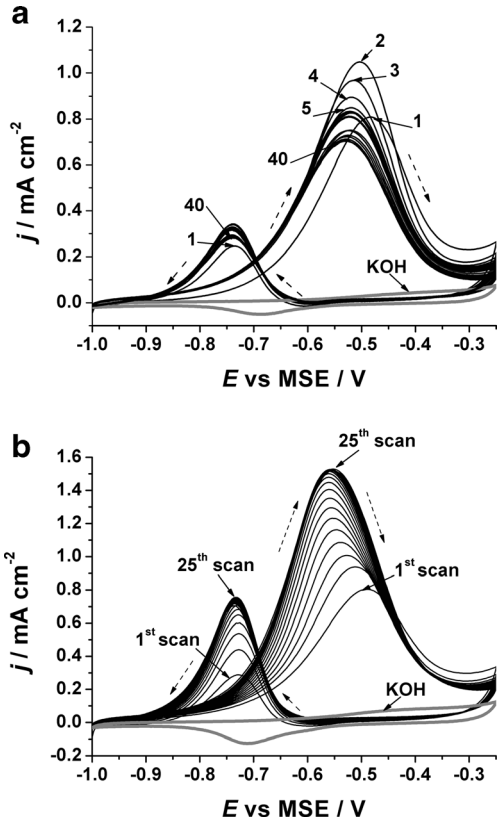

Fig. 5 Series of cyclic voltammetric curves of glycerol oxidation measured in 0.1 mol cm^{-3} glycerol and 0.5 mol cm^{-3} KOH solution on Pd/PEDOT layers obtained by **a** single-step and **b** triple-step Pd deposition. *Gray line* denotes the measurement in absence of glycerol. Scan rate $v = 0.02$ V s^{-1}

100 % from the initial value (Fig. 5b). It is worth noting that at a higher scan rate and higher glycerol concentration, an even stronger increase of the main peak current is observed in the course of voltammetric scanning (Fig. 6). These different trends in the voltammetric behavior can be discussed in the context of following investigations. In a recent work [18], it

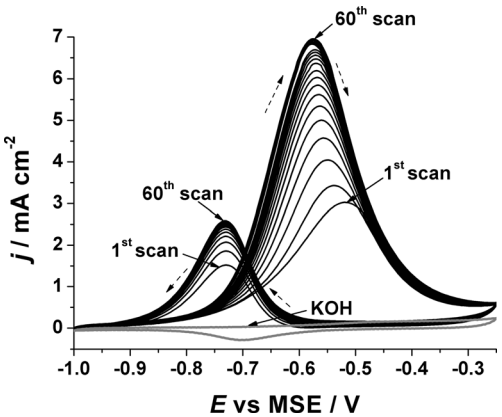

Fig. 6 Series of cyclic voltammetric curves for glycerol oxidation measured in 0.5 mol cm^{-3} glycerol and 0.5 mol cm^{-3} KOH at Pd/PEDOT obtained by triple-step Pd deposition. *Gray line* denotes the measurement in absence of glycerol. Scan rate $v = 0.05$ V s^{-1}

was shown that repetitive oxidation/reduction of the electrocatalyst consisting of small Pd NPs (8.4 nm) in 2 M KOH with and without ethanol results in deactivation of the Pd catalysts due to the formation of surface PdO. The so-called anodic stress of the Pd electrocatalyst [18] was found to depend strongly on the positive potential limit used in the experiment. The electrochemistry of Pd NPs deposited on glassy carbon electrode was extensively studied in neutral and alkaline solutions [46]. Pd NPs size-dependent redox potential was suggested to explain pre-monolayer oxide formation at more negative potentials than expected for the Pd bulk phase. On the other hand, a repetitive electrochemical redox treatment (with very high positive potential limit) of polycrystalline Pd surface was found to enhance the electrocatalytic response for ethanol, ethylene glycol, and glycerol oxidation [9]. Furthermore, it was reported that Pd (111) surface can be re-ordered by multiple sequences of electrochemical surface oxidation and reduction followed by several cycles of

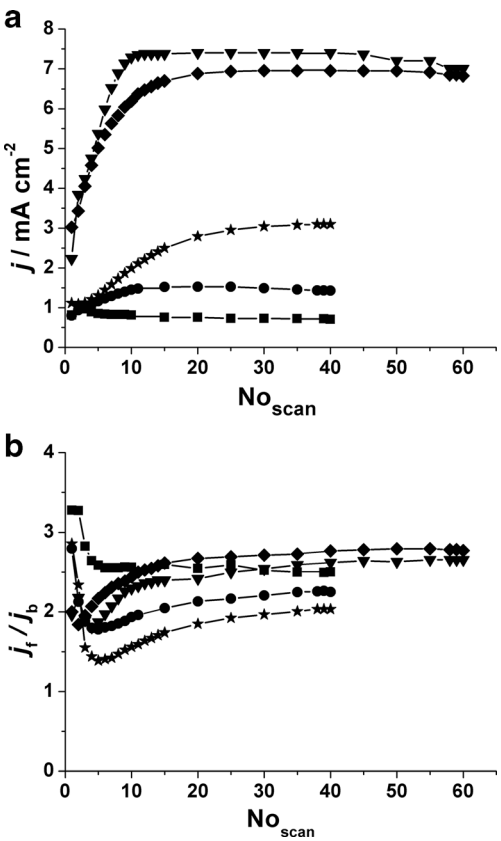

Fig. 7 Dependence of **a** cyclic voltammetric forward peak current and **b** the forward to backward current peak ratio on the number of consecutive voltammetric scans at Pd-PEDOT specimens obtained at different conditions: single-step (*filled squares*) and triple-step (*filled circles*, *stars*, *diamonds*, and *down-pointing triangles*) Pd deposition; 0.1 mol cm^{-3} (*filled squares*, *circles*, and *stars*) and 0.5 mol cm^{-3} (*filled diamonds* and *down-pointing triangles*) glycerol; scan rates $v = 0.02$ V s^{-1} (*filled squares* and *circles*) and $v = 0.05$ V s^{-1} (*filled stars*, *diamonds*, and *down-pointing triangles*) (see Table 1)

Table 2 Comparative data for the mass activity and forward-to-backward peak current ratio for glycerol oxidation obtained with Pd-based electrocatalysts

Pd catalyst	Solution	*MA* (j/m_{Pd}) (mA mg^{-1})	j_f/j_b	Reference
Voltammetric experiments				
Pd dendrites/PEDOT	1.0 mol cm^{-3} NaOH 0.1 mol cm^{-3} glycerol 0.05 V s^{-1}	100	2.5	[25]
Pd/PANI; Pd/TiO_2-PANI	0.5 mol cm^{-3} KOH 0.1 mol cm^{-3} glycerol 0.02 V s^{-1}	300	3.7; 5.5	[22]
Pd black; 10 % Pd/C; Pd/RGO	0.5 mol cm^{-3} KOH 0.5 mol cm^{-3} glycerol 0.025 V s^{-1}	23.2; 4.0; 25.1	1.1; 3.0; 3.0	[17]
Pd/NPSS; Pd/Cu/NPSS	1 mol cm^{-3} KOH 5 % wt.% glycerol 0.05 V s^{-1}	20; 82	n.d.	[13]
Pd/C; FeCo@Fe@Pd/C	0.5 mol cm^{-3}KOH 0.5 mol cm^{-3} glycerol 0.025 V s^{-1}	52; 259	4.73; 2.8	[16]
Pd/C; Pd@WC-Mo_2C aerogel supports	0.5 mol cm^{-3}KOH 0.5 mol cm^{-3} glycerol 0.05 V s^{-1}	800; 1700–2050 (for various supports)		[12]
Pd/PEDOT	0.5 mol cm^{-3} KOH 0.5 mol cm^{-3} glycerol 0.05 V s^{-1}	720	2.8	This work
Chronoamperometric experiments				
Pd/NPSS; Pd/Cu/NPSS	1 mol cm^{-3} KOH 5 % wt.% glycerol $E = -0.2$ V vs. Ag/AgCl	0.8; 13.8		[13]
Pd/C; FeCo@Fe@Pd/C	0.5 mol cm^{-3} KOH 0.5 mol cm^{-3}glycerol $E = -0.2$ V vs. Ag/AgCl	≈3; 37		[16]
10 % Pd/C; Pd/RGO	0.5 mol cm^{-3} KOH 0.5 mol cm^{-3} glycerol $E = -0.3$ V vs. SCE	≈0.8; 1.5		[17]
Pd-PEDOT	0.5 mol cm^{-3} KOH 0.5 mol cm^{-3} glycerol $E = -0.6$ V vs. MSE	97; 47 (after 60 CV cycles)		this work

RGO reduced graphene oxide, *NPSS* nanoporous stainless steel

oxidative chemisorption and reductive desorption of iodine [47] but possibly also of other species.

In the present studies, NPs obtained upon single deposition step are small (12 nm in diameter on the average) and "anodic-stress" type of deactivation may be expected as in the case of the Pd NPs with similar size studied in [18]. The larger particles deposited in the triple-step electroless deposition experiment seem to be stable and provide increasing electroactivity upon repeated oxidation/reduction similar to the result obtained in [9]. The same effect was observed in our former studies on temperature-treated Pd-PANI electrocatalysts [22]. This may occur if surface restructuring takes place upon consecutive Pd surface oxide formation/reduction, thus providing the possibility to expose crystalline faces with better electrocatalytic activity for the studied oxidation reaction.

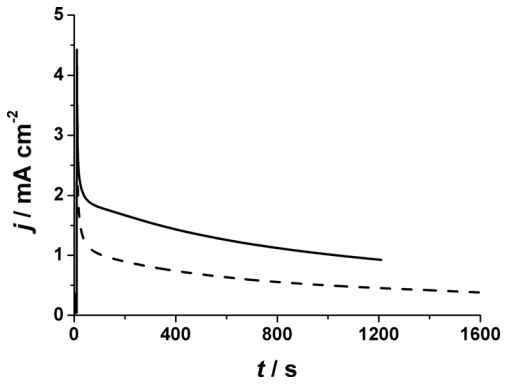

Fig. 8 Chronoamperometric curves measured at constant potential ($E = -0.6$ V) in 0.5 mol cm^{-3} and 0.5 mol cm^{-3} KOH at Pd-PEDOT specimen (triple step Pd deposition) before (*solid line*) and after (*dashed line*) 60 voltammetric scans in the same solution

One of the most important points concerning the use of CP-based electrocatalysts in practical applications is their stability. It is usually assessed by multiple voltammetric cycling or chronoamperometric experiments. A comparison of the data obtained by voltammetric experiments at Pd-PEDOT specimens investigated at different conditions (i.e., scan rate and glycerol concentration) is presented in Fig. 7. The data for the forward glycerol oxidation peak current in dependence on the number of scans (Fig. 7a) show that steady-state values are reached within the first ten scans if working at the higher glycerol concentration (0.5 mol cm^{-3}) and the higher scan rate (0.05 V s^{-1}) (see triangles in the figure). A comparison of the voltammetric behavior of Pd-PEDOT specimens (triple step deposition) used for voltammetric studies before (triangles)

and after (rhombuses) a chronoamperometric measurement is also presented in Fig. 7a. In the latter case, the steady state is attained more slowly, indicating possible surface contamination of the Pd catalyst that occurred in the course of the chronoamperometric experiment. At lower concentrations of glycerol and lower scan rate, the electrodes need a larger number of scans for conditioning. The data for the mass electroactivity ($MA = j_f/m_{Pd}$) of the investigated Pd-PEDOT specimens are given in Table 1. In comparison to the mass electroactivity of other Pd-based electrocatalysts [13, 16, 17, 25], tested at the comparable conditions, the value obtained here, $j_f/m_{Pd} = 720$ mA mg^{-1}, is markedly higher (Table 2). A similar value for *MA* is communicated for Pd NPs supported on carbon powder [12] whereas markedly higher values were obtained when using complex binary carbide and carbon aerogel composites as support for Pd [12]. No data for the stability of the catalyst were presented in the latter case.

An important indication for the effectiveness of the glycerol oxidation process is the forward-to-backward peak current ratio, j_f/j_b (Fig. 7b). For the higher glycerol concentration (0.5 mol cm^{-3}), the ratio j_f/j_b takes a steady-state value close to 3. Such a value was observed for an electrocatalyst obtained by preparation of Pd nanodendrites anchored in reduced graphene oxide [17]. The difference, however, is that the value of *MA* obtained here is much higher, 750 vs. 25 mA mg^{-1} [17]. Higher values of the j_f/j_b ratio were obtained in other studies [16, 22] but again at a lower electrocatalytic mass activity (Table 2).

Finally, Fig. 8 shows chronoamperometric measurements at Pd-PEDOT (triple electroless deposition) in glycerol-containing solution before and after continuous voltammetric cycling. After an initial steep decrease, both transients show relatively stable behavior although the transient obtained after continuous cycling in glycerol has lower current values. This means that irreversible contamination of the Pd catalysts takes place in the course of continuous cycling. Nevertheless, the obtained steady-state *MA* values are higher than those so far reported in the literature under comparable conditions (Table 2).

Conclusions

The present investigation addresses the possibility to obtain stable and effective Pd-based catalysts by using electroless Pd deposition at the expanse of PEDOT oxidation. Experiments carried out at single- and triple-step metal deposition demonstrate the possibility to vary the mean size of deposited NPs by achieving homogeneous surface distribution of the metallic phase. It is established that the Pd-PEDOT electrocatalyst with small Pd NPs (estimated mean size of about 12 nm) loses its initial electroactivity. In contrast, when depositing larger Pd NPs ($d \approx 20$ nm), the electroactivity increases significantly within the first 20 voltammetric cycles followed by a stable behavior. The proposed method of dispersing the Pd catalytic phase provides the opportunity to work with small Pd loadings (up to 10 μg cm^{-2}). The *MA* for electrooxidation of glycerol established at these loadings is between the highest values achieved at Pd catalysts without additional modification (e.g., deposition of a second metal) of the electrocatalytic phase. It is worth noting that the proposed approach for the preparation of the Pd catalysts may be further extended to electroless deposition of a second metal (e.g., Ag) in order to obtain bi-metallic catalysts with improved performance.

Finally, the present investigation shows also a very good electrochemical stability of PEDOT in alkaline solutions. The initial intrinsic electroactivity of PEDOT (obtained after synthesis) was almost completely restored after a series of continuous measurements in glycerol and even after the dissolution of Pd. This observation is in contrast with findings showing a severe degradation of PEDOT in the course of voltammetric cycling in alkaline solution [48]. The discrepancy should be sought in the different positive potential limits used in the two investigations. A less positive potential limit ($E = -0.25$ V) as the one used throughout the present experiments seems not be harmful for PEDOT as support for the catalytic phase.

References

1. Corti, Horacio R, Gonzalez, Ernesto R (eds) (2013) Direct alcohol fuel cells. Materials, performance, durability and applications. Springer
2. Antolini E, Gonzalez ER (2009) Polymer supports for low-temperature fuel cells. Appl Catal A 365:1–19
3. Bianchini C, Shen PK (2009) Palladium-based electrocatalysts for alcohol oxidation in half cells and in direct alcohol fuel cells. Chem Rev 109:4183–4206
4. Antolini E, Zignani SC, Santos SF, Gonzalez ER (2011) Palladium-based electrodes: a way to reduce platinum content in polymer-electrolyte membrane fuel cells. Electrochim Acta 56:2299–2305
5. Yildiz G, Kadirgan F (1994) Electrocatalytic oxidation of glycerol. Behavior of palladium electrode in alkaline medium. J Electrochem Soc 141:725–730
6. Bambagioni V, Bianchini C, Marchionni A, Filippi J, Vizza F, Teddy J, Serp P, Zhiani M (2009) Pd and Pt-Ru anode electrocatalysts supported on multiwalled carbon nanotubes and their use in passive and active direct alcohol fuel cells with an anion-exchange membrane (alcohol = methanol, ethanol, glycerol). J Power Sources 190:241–251
7. Simoes M, Baranton S, Coutanceau C (2010) Electro-oxidation of glycerol at Pd based nano-catalysts for an application in alkaline fuel cells for chemicals and energy cogeneration. Appl Catal B Environ 93:354–362
8. Habibi E, Razmi H (2012) Glycerol electrooxidation on Pd, Pt and Au nanoparticles supported on carbon ceramic electrode in alkaline medium. Int J Hydrog Energy 37:16800–16809
9. Wang L, Bevilicqua M, Chen YX, Filippi J, Innocenti M, Lavacchi A, Marchionni A, Miller H (2013) Enhanced electrooxidation of

alcohols at electrochemically treated polycrystalline palladium surface. J Power Sources 242:872–876
10. Zhang Z, Xin L, Qi J, Chadderdon DJ, Li W (2013) Supported Pt, Pd and Au nanoparticle anode catalysts for anion-exchange membrane fuel cells with glycerol and crude glycerol fuels. Appl Catal B 136–137:29–39
11. Machado BF, Marchionni A, Basca RR, Bellini M, Beausoleil J, Oberhauser W, Vizza F, Serp P (2013) Synergistic effect between few layer grapheme and carbon nanotubes supports for palladium catalyzing electrochemical oxidation of alcohols. J Energy Chem 22:296–304
12. Zhang X, Shen PK (2013) Glycerol oxidation on highly active Pd supported carbide/C aerogel composite catalysts. Int J Hydrogen Energy 38:2257–2262
13. Rezaei B, Havakeshian E, Ensafi AA (2014) Fabrication of porous Pd film on nanoporous stainless steel using galvanic replacement as a novel electrocatalyst/electrode design for glycerol oxidation. Electrochim Acta 136:89–96
14. Renard D, McCain C, Baidoun B, Bondy A, Bandyopadhay K (2014) Electrocatalytic properties of in-situ generated assemblies towards oxidation of multi-carbon alcohols and polyalcohols. Colloids Surf A 463:44–54
15. Sadiki A, Vo P, Hu S, Copenhaver TS, Scudiero L, Ha S, Haan JL (2014) Increased electrochemical oxidation rate of alcohols in alkaline media on palladium surfaces electrochemically modified by antimony, lead and tin. Electrochim Acta 139:302–307
16. Fashedemi OO, Ozoemena KI (2014) Comparative electrocatalytic oxidation of ethanol, ethylene glycol and glycerol in alkaline medium at Pd-decorated FeCo@Fe/C core-shell nanocatalysts. Electrochim Acta 128:279–286
17. Li SS, Hu YY, Feng JJ, Lv ZY, Chen JR, Wang AJ (2014) Rapid room-temperature synthesis of Pd nanodendrites on reduced graphene oxide for catalytic oxidation of ethylene glycol and glycerol. Int J Hydrog Energy 39:3730–3738
18. Wang L, Lavacchi A, Bellini M, D'Acapito F, Benedetto FD, Innocenti M, Miller HA, Montegrossi G, Zafferoni C, Vizza F (2015) Deactivation of palladium electrocatalysts for alcohols oxidation in basic electrolytes. Electrochim Acta 177:100–106
19. Hatchett DW, Millick NM, Kinyanjui JM, Pookpanratana S, Baer M, Hofmann T, Luinetti A, Heske C (2011) The electrochemical reduction of $PdCl_4^{2-}$ and $PdCl_6^{2-}$ in polyaniline: influence of Pd deposit morphology on methanol oxidation in alkaline solution. Electrochim Acta 56:6060–6070
20. Zhao ZL, Tian J, Nie S, Ning Z (2011) Enhanced electrocatalytic oxidation of methanol on Pd/polypyrrole-graphene in alkaline. Electrochim Acta 56:1967–1972
21. Ghosh S, Teilout AL, Floresyona D, de Oliveira P, Hagege A, Remita H (2015) Conducting polymer-supported palladium nanoplates for applications in direct alcohol oxidation. Int J Hydrog Energy 40:4951–4959
22. Ilieva M, Tsakova V (2015) Temperature-treated polyaniline layers as support for Pd catalysts: electrooxidation of glycerol in alkaline medium. J Solid State Electrochem 19:2811–2818
23. Pandey RK, Lakshminarayanan V (2010) Enhanced electrocatalytic activity of Pd-dispersed 3,4-polyethylenedioxythiophene film in hydrogen evolution and ethanol electro-oxidation reactions. J Phys Chem C 114:8507–8514
24. Jiang F, Yao Z, Yue R, Xu J, Du Y, Yang P, Wang C (2013) Electrocatalytic activity of Pd nanoparticles supported on poly(3,4-ethylenedioxy-thiophene)-graphene hybrid for ethanol electrooxidation. J Solid State Electrochem 17:1039–1047
25. Dash S, Munichandraiah N (2012) Electrocatalytic oxidation of 1,2-propanediol on electrodeposited Pd–poly(3,4-ethylenedioxythiophene) nanodendrite films in alkaline medium. Electrochim Acta 80:68–76
26. Dash S, Munichandraiah N (2013) Electrocatalytic oxidation of C3-aliphatic alcohols on electrodeposited Pd-PEDOT nanodendrites in alkaline medium. J Electrochem Soc 160:H197–H202
27. Dash S, Munichandraiah N (2015) Nanoflowers of PdRu on PEDOT for electrooxidation of glycerol and its analysis. Electrochim Acta. doi:10.1016/j.electacta.2015.07.020
28. Yue R, Wang H, Bin D, Xu J, Du Y, Lu W, Guod J (2015) Facile one-pot synthesis of Pd-PEDOT/graphene nanocomposites with hierarchical structure and high electrocatalytic performance for ethanol oxidation. J Mater Chem A 3:1077–1088
29. Tsakova V (2010) Metal-based composites of conducting polymers. In: Eftekhari A (ed) Nanostructured conductive polymers. John Wiley & Sons, ISBN 978-0-470-74585-4, p. 289–340.
30. Kondratiev VV, Malev VV, Eliseeva SN (2016) Composite electrode materials based on conducting polymers loaded with metal nanostructures. Russ Chem Rev 85:14–37
31. Mourato A, Viana AS, Correia JP, Siegenthaler H, Abrantes LM (2004) Polyaniline films containing electrolessly precipitated palladium. Electrochim Acta 49:2249–2257
32. Lyutov V, Tsakova V (2011) Palladium-modified polysulfonic acid-doped polyaniline layers for hydrazine oxidation in neutral solutions. J Electroanal Chem 661:186–191
33. Moghaddam RB, Pickup PG (2011) Formic acid oxidation at spontaneously deposited palladium on polyaniline modified carbon paper. Electrochim Acta 56:7666–7672
34. Ilieva M, Tsakova V, Erfurth W (2006) Electrochemical formation of bi-metal (copper-palladium) electrocatalyst supported on poly-3,4-ethyelenedioxythiophene. Electrochim Acta 52:816–824
35. Eliseeva SN, Malev VV, Kondratiev VV (2009) Electrochemical properties of composite films based on poly-3,4-ethylenedioxythiophene with inclusions of metallic palladium. Russ J Electrochem 45:1045–1051
36. Eliseeva SN, Ubyivovk EV, Bondarenko AS, Vyvenko OF, Kondratiev VV (2010) Synthesis and structure of poly-3,4-ethylenedioxythiophene film with the inclusions of palladium nanoparticles. Russ J Gen Chem 80:1143–1148
37. Kondratiev VV, Babkova TA, Eliseeva SN (2012) Structure and electrochemical properties of composite films based on poly-3,4-ethylenedioxythiophene with metallic palladium inclusions. Russ J Electrochem 48:205–211
38. Kondratiev VV, Babkova TA, Tolstopjatova EG (2013) PEDOT-supported Pd nanoparticles as a catalyst for hydrazine oxidation. J Solid State Electrochem 17:1621–1630
39. Quispe CAG, Coronado CJR, Carvalho JA Jr (2013) Glycerol: production, consumption, prices, characterization and new trends in combustion. Renew Sust Energy Rev 27:475–493
40. Grden M, Lukazsewski M, Jerkiewicz G, Czerwinski A (2008) Electrochemical behavior of palladium electrode: oxidation, electrodissolution and ionic adsorption. Electrochim Acta 53:7583–7598
41. Macfie G, Cooper A, Cardosi MF (2011) Room temperature formation, electro-reduction and dissolution of surface oxide layers on sputtered palladium films. Electrochim Acta 56:8394–8402
42. Morvant MC, Reynolds JR (1998) In situ conductivity study of poly(3,4-ethylenedioxythiophene). Synth Met 92:57–61
43. Lapkowski M, Pron A (2000) Electrochemical oxidation of poly(3,4-ethylenedioxythiophene)—in situ conductivity and spectroscopic investigations. Synth Met 110:79–83
44. Genesca J, Duran R (1987) The effect of Cl^- on the kinetics of the anodic dissolution of Pd in H_2SO_4 solutions. Electrochim Acta 32:541–544
45. Atgelt KH, Boduszynski MM (1994) Composition and analysis of heavy petroleum fractions. Marcel Dekker, New York, p 214, Chapter 6
46. Diculescu VC, Chiorcea-Paquim AM, Corduneanu O, Oliveira-Brett AM (2007) Palladium nanoparticles and nanowires deposited electrochemically: AFM and electrochemical characterization. J Solid State Electrochem 11:887–898

47. Bothwell ME, Cali GJ, Berry GM, Soriaga MP (1991) In situ regeneration of clean and ordered Pd (111) electrode surfaces by oxidative chemisorption and reductive desorption of iodine. Surf Sci Lett 249:322–326

48. Zanfrognini B, Colina A, Heras A, Zanardi C, Seeber R, Lopes-Palacios J (2011) A UV-Visible/Raman spectroelectrochemical study of the stability of poly(3,4-ethylendioxythiophene) films. Polym Degrad Stab 56:2112–2119